*Osteoarthritis and Cartilage* (2009) **17,** 714–722

doi:10.1016/j.joca.2008.11.017

**Osteoarthritis and Cartilage**

International Cartilage Repair Society

OARSI OSTEOARTHRITIS RESEARCH SOCIETY INTERNATIONAL

# Repair of full-thickness femoral condyle cartilage defects using allogeneic synovial cell-engineered tissue constructs[1]

M. Pei†‡*, F. He†‡, B. M. Boyce† and V. L. Kish†

† *Tissue Engineering Laboratory, Department of Orthopaedics, West Virginia University, Morgantown, WV 26506, USA*

‡ *Division of Exercise Physiology, West Virginia University, Morgantown, WV 26506, USA*

## Summary

*Objective*: Synovium-derived stem cells (SDSCs) have proven to be superior in cartilage regeneration compared with other sources of mesenchymal stem cells. We hypothesized that conventionally passaged SDSCs can be engineered *in vitro* into cartilage tissue constructs and the engineered premature tissue can be implanted to repair allogeneic full-thickness femoral condyle cartilage defects without immune rejection.

*Methods*: Synovial tissue was harvested from rabbit knee joints. Passage 3 SDSCs were mixed with fibrin glue and seeded into non-woven polyglycolic acid (PGA) mesh. After 1-month incubation with growth factor cocktails, the premature tissue was implanted into rabbit knees to repair osteochondral defects with Collagraft® as a bone substitute in the Construct group. Fibrin glue-saturated PGA/Collagraft® composites were used as a Scaffold group. The defect was left untreated as an Empty group.

*Results*: SDSCs were engineered in rotating bioreactor systems into premature cartilage, which displayed the expression of sulfated glycosaminoglycan (GAG), collagen II, collagen I, and macrophages. Six months after implantation with premature tissue, cartilage defects were full of smooth hyaline-like cartilage with no detectable collagen I and macrophages but a high expression of collagen II and GAG, which were also integrated with the surrounding native cartilage. The Scaffold and Empty groups were resurfaced with fibrous-like and fibrocartilage tissue, respectively.

*Conclusion*: Allogeneic SDSC-based premature tissue constructs are a promising stem cell-based approach for cartilage defects. Although *in vitro* data suggest that contaminated macrophages affected the quality of SDSC-based premature cartilage, effects of macrophages on *in vivo* tissue regeneration and integration necessitate further investigation.


*Key words*: Synovium, Mesenchymal stem cell, Tissue engineering, Cartilage defect, Repair, Allograft.

## Introduction

Once damaged, articular cartilage has only limited intrinsic capacity for self-repair[1,2]. Although autologous chondrocyte implantation (ACI) has some advantages, a general problem with this chondrocyte-based procedure in cartilage repair is the quality of newly formed cartilage. For example, implanted chondrocytes undergo hypertrophic differentiation with subsequent ossification[3,4] and poor integration to host tissue[5,6]. In contrast, it has been shown that immature constructs using mesenchymal stem cells (MSCs) integrate better and are more durable[7–9]. MSCs can regenerate not only cartilage but also the underlying subchondral bone[10] and are therefore able to resurface osteochondral defects as well.

MSCs are characterized by their multipotentiality and capacity for self-renewal[11]. The hypoimmunogenic nature implies that MSCs can be used in allogeneic cell-based therapy[12,13]. MSCs from different sources have exhibited different properties in expansion capacity and multi-lineage differentiation[14]. Synovium-derived stem cells (SDSCs) are a promising source of stem cells for cartilage tissue engineering because they display greater chondrogenic and less osteogenic potential than MSCs derived from bone marrow or periosteum[15]. They are also proven to be superior to other sources of MSCs such as adipose tissue and muscle[16–18]. Under appropriate stimulation conditions, they are able to migrate into articular cartilage defects and subsequently undergo chondrogenic differentiation[10,19]. Studies also show that the molecular profile of SDSCs is stable during *in vitro* expansion from passage 3 up to at least passage 10[20,21].

Imitating the involvement of growth factors in cartilage development, our previous study characterized the properties of SDSCs and defined growth factor cocktails for maximal cell proliferation and chondrogenic differentiation[22]. However, it is unknown whether SDSCs can be engineered into cartilage-like tissue in bioreactor systems supplemented with growth factor cocktails. We also question if allogeneic SDSC-engineered premature tissue can be implanted to repair full-thickness femoral condyle cartilage defects without immune rejection. Although MSCs have immune "privilege" and immunomodulatory capacity, the implanted tissue constructs derived from allogeneic SDSCs

[1]Supported by a grant from the Musculoskeletal Transplant Foundation (MTF) to M.P.

*Address correspondence and reprint requests to: M. Pei, Tissue Engineering Laboratory, Department of Orthopaedics, West Virginia University, PO Box 9196, One Medical Center Drive, Morgantown, WV 26506-9196, USA. Tel: 1-304-293-1072; Fax: 1-304-293-7070; E-mail: mpei@hsc.wvu.edu

Received 30 June 2008; revision accepted 28 November 2008.

having partially differentiated into chondrocytes. Therefore, we are unsure whether the differentiated MSCs still have immunomodulatory properties.

We hypothesized that SDSCs can be engineered *in vitro* into cartilage tissue constructs and allogeneic SDSC-engineered premature tissue can be implanted to repair full-thickness femoral condyle cartilage defects without immune rejection. Our long-term goal is to engineer high-quality cartilage constructs using allogeneic SDSCs for the repair of cartilage defects resulting from trauma and osteoarthritis.

## Materials and methods

### SDSC ISOLATION AND CULTURE

Random biopsies of synovial tissue were obtained aseptically from the knees of two 8-month-old New Zealand white rabbits and pooled together [Fig. 1(A)]. The synovial tissue was finely minced and digested at 37°C for 30 min in phosphate-buffered saline (PBS) containing 0.1% trypsin and then for 2 h in 0.1% solution of collagenase P in DMEM/10% fetal bovine serum (FBS). After passing through a 70-μm nylon filter, the cells were collected from the filtrate by centrifugation. Cells were plated and cultured for 4 days in complete medium (DMEM/F12/10% FBS, 100 U/mL penicillin, 100 μg/mL streptomycin). Non-adherent cells were removed by a PBS wash on days 2 and 4. After 90% confluence, primary cells were trypsinized and replated as passage 1. Passage 3 SDSCs were collected for this study [Fig. 1(B)].

### *IN VITRO* ENGINEERED SDSC-BASED TISSUE CONSTRUCTS

Degradable polyglycolic acid (PGA) scaffolds (a mesh of 15-μm fibers and 97% void volume; Synthecon, Houston, TX) were punched into 5-mm-diameter × 2-mm-thick discs and sterilized with ethylene oxide, then immersed in 100% ethanol, 70% ethanol, and PBS (without $Ca^{2+}$ and $Mg^{2+}$). In a centrifuge tube, 150 μL fibrinogen (100 mg/mL in PBS, Sigma, St. Louis, MO) [Fig. 1(C)], 140 μL PBS with cells, 5 μL thrombin (0.1 U/μL, Sigma), and 5 μL $CaCl_2$ (50 mM) were sequentially added. Then, 26 μL of SDSC-gel mixture was pipetted onto a PGA disc [Fig. 1(D)] in a Petri dish. This procedure resulted in a total of 56 fibrin-PGA composites containing $2.6 \times 10^6$ cells per scaffold [Fig. 1(E)], corresponding to an initial seeding density of $100 \times 10^6$ cells/mL. The dish with constructs was transferred into an incubator for 10 min. Complete medium was then added to cover the constructs.

After 1 h, the medium was replaced by chemically defined medium (high-glucose DMEM, 40 μg/mL proline, 100 nmol/L dexamethasone, 0.1 mmol/L ascorbic acid 2-phosphate, 100 U/mL penicillin, 100 μg/mL streptomycin, and 1 × ITS™ Premix) supplemented with a proliferative growth factor cocktail (10 ng/mL transforming growth factor β1 [TGF-β1], 50 ng/mL basic fibroblast growth factor [FGF-2], and 500 ng/mL insulin-like growth factor I [IGF-I]) for 3 days [Fig. 1(F)][22]. The cell-fibrin-PGA constructs were transferred to a rotating bioreactor (Rotary Cell Culture System-4 (RCCS-4); Synthecon) filled with chemically defined medium supplemented by a differentiative growth factor cocktail (10 ng/mL TGF-β1 and 500 ng/mL IGF-I) for 28 days [Fig. 1(G)][22] The bioreactor rotation speed was adjusted to maintain the growing constructs freely suspended in the rotating flow. Forty-four tissue constructs were harvested [Fig. 1(H)] for the analyses at days 0, 3, 15, and 31. Another 12 1-month constructs were used for *in vivo* implantation.

### *IN VIVO* IMPLANTATION OF PREMATURE TISSUE FOR CARTILAGE REPAIR

This project was approved by the Institutional Animal Care and Use Committee (IACUC) and conducted in compliance with the National Advisory Committee for Laboratory Animal Research Guidelines. Eighteen New Zealand white rabbits (8-month-old males weighing 3.5–4.0 kg) (Covance, Denver, PA) were used in this study. The rabbits were anesthetized with 5 mg/kg xylazine (Phoenix Pharmaceutical, St. Joseph, MO) and 35 mg/kg ketamine (Phoenix Pharmaceutical) intramuscularly and maintained with isofluorane. The knee joints were approached through medial parapatellar incisions and the articular surfaces were exposed by lateral dislocation of the patellae. Full-thickness osteochondral defects, 4 mm diameter × 5 mm deep, were

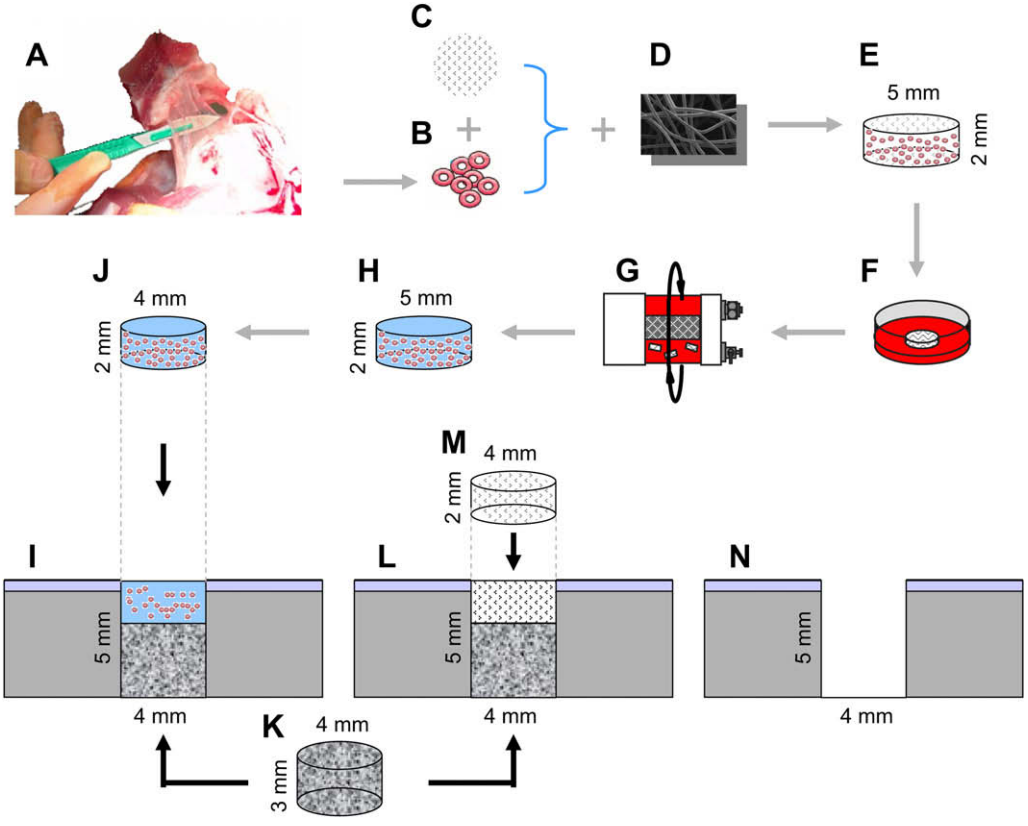


Fig. 1. Diagram illustrating research design. (A): Synovial tissue harvesting. (B): SDSCs. (C): Fibrin glue. (D): PGA disc. (E): Cell-fibrin glue-PGA construct. (F): Static culture (3 days). (G): Bioreactor culture (4 weeks). (H): Premature tissue construct. (I): Construct group. (J): Punched tissue construct. (K): Fibrin glue-saturated Collagraft®. (L): Scaffold group. (M): Fibrin glue-saturated PGA scaffold. (N): Empty group.

created in the medial femoral condyles of both knees using a dental drill (Henry Schein, Melville, NY) with a depth stop.

Our experimental design included three groups: ''Construct'', ''Scaffold'', and ''Empty''. In the Construct group [Fig. 1(I)], 12 defects were filled randomly with punched tissue constructs [Fig. 1(J)] with fibrin glue-saturated Collagraft® (Zimmer, Warsaw, IN) as a bone substitute [Fig. 1(K)]. In the Scaffold group [Fig. 1(L)], 12 defects were filled with fibrin glue-saturated PGA [Fig. 1(M)]/Collagraft® composites. In the Empty group [Fig. 1(N)], 12 defects were left untreated. All rabbits were returned to their cages after the operation and allowed to move freely. Animals were sacrificed by an intracardiac puncture of Euthasol® euthanasia solution (Fort Dodge Animal Health, Fort Dodge, IA) at 3 weeks ($n = 3$) and 6 months ($n = 15$) after the operation. The femoral condyles were isolated for histomorphological analysis.

### HISTOLOGICAL ANALYSIS

Tissue constructs ($n = 3$) were fixed overnight at 4°C in 4% paraformaldehyde in PBS. For the implantation study, the dissected distal femurs were also decalcified at 4°C in 4% ethylene-diamine-tetra-acetic acid (EDTA) solution on a shaker. Radiographs were used to evaluate the progress of decalcification. After decalcification, the samples were dehydrated with a gradient ethanol series, cleared with xylene, and embedded in paraffin blocks. Sagittal sections were cut at 5 μm thickness. The sections were routinely stained with hematoxylin and eosin (H&E). To differentiate between cartilage and fibrous tissue, combined Safranin-O/fast green staining was performed. All evaluations were performed at the most central section of the halved defect specimen to ensure unbiased analysis.

All samples were also immunostained with monoclonal antibodies against collagen II (II-II6B3; DSHB, Iowa City, IA), collagen I (Abcam, Cambridge, MA), and macrophage Ab-5 (Clone RAM11, Lab Vision, Fremont, CA). Immunohistochemical sections were deparaffinized using xylene and hydrated through graded alcohols. The samples were pretreated with 1% hydrogen peroxide and incubated for 30 min with 2 mg/mL testicular hyaluronidase in PBS (pH 5) at 37°C followed by another 30 min with 1.5% normal goat serum and overnight at 4°C with the primary antibody. After extensive washing with PBS, a secondary antibody of biotinylated horse anti-mouse IgG (Vector, Burlingame, CA) was placed on the sections for 30 min at room temperature. Immunostaining was conducted with Vectastain ABC reagent (Vector) followed by 3,3′-diaminobenzidine (DAB) staining. Counterstaining was performed with hematoxylin (Vector).

### SEMIQUANTITATIVE HISTOLOGICAL SCORING

Two observers blinded to the treatment groups evaluated the sections according to the histological grading scale[23,24]. Five categories, including cell morphology, matrix staining, surface regularity, thickness of cartilage, and integration with adjacent host cartilage, were examined with a maximum score of 14 being the poorest result. This evaluation was performed according to the ''Modified Histological Grading Score'', which also included unfilled defects[25]. The total scores were compared among experimental groups.

### BIOCHEMICAL ANALYSIS

Tissue constructs ($n = 4$) from the *in vitro* bioreactor culture were digested for 6 h at 60°C with 125 μg/mL papain in PBE buffer (100 mmol/L phosphate, 10 mmol/L EDTA, pH 6.5) containing 10 mmol/L cysteine, using 100 μL enzyme per sample. To quantify cell density, the amount of deoxyribonucleic acid (DNA) in the papain digests was measured using the Quant-iT™ PicoGreen® dsDNA Assay kit (Invitrogen, Carlsbad, CA) with a CytoFluor® Series 4000 (Applied Biosystems, Foster City, CA). GAG content was measured using dimethylmethylene blue dye (DMMB) and a Spectronic™ BioMate™ 3 Spectrophotometer (Thermo Scientific, Milford, MA)[26].

### WESTERN BLOT

To assess collagen II expression, tissue constructs ($n = 3$) were lyophilized, measured for dry weights, incubated using 50 mg dry sample per 15 mL 4 mol/L guanidine hydrochloride (Sigma) for 20 h at 4°C, homogenized, and digested with 0.6 mg/mL of pepsin (Sigma) per mL in 0.5 mol/L acetic acid (Sigma) at 4°C for 48 h at a 10:1 ratio of dry sample to pepsin (mg/mg). The samples were centrifuged at 48,000 g for 1 h, and the supernatant was lyophilized and dissolved in radioimmunoprecipitation assay (RIPA, Pierce, Rockford, IL) buffer with protease inhibitors (Roche, Indianapolis, IN). To assess Sox 9 protein expression, the samples were homogenized and dissolved in RIPA buffer with protease inhibitors. Total proteins were quantified using BCA™ Protein Assay Kit (Pierce). The samples were denatured and separated by NuPAGE® Novex® Bis-Tris Mini Gels (Invitrogen) in the XCell SureLock™ Mini-Cell (Invitrogen) at 120 V for 3 h at 4°C. Bands were transferred onto a nitrocellulose membrane (Invitrogen) using XCell II™ Blot module (Invitrogen) at 15 V overnight at 4°C. Nonspecific binding was blocked with 5% nonfat milk in TBST (100 mmol/L Tris-HCl, 0.9% NaCl, 1% Tween® 20, pH 7.5) for 1 h. The membrane was incubated with a primary monoclonal antibody in 1% nonfat milk in TBST to collagen II (DSHB) or Sox 9 (Abcam) for 1 h at room temperature (β-actin served as an internal control for Sox 9), followed by the secondary antibody of horseradish peroxidase-conjugated goat anti-mouse (Pierce) for 40 min at room temperature and exposure using SuperSignal® West Femto Maximum Sensitivity Substrate (Pierce) and CL-XPosure™ Film (Pierce). For semi-quantitative analysis, bands were scanned (CanoScan8400F, Canon, Lake Success, NY) and analyzed using NIH Image J software (US National Institutes of Health, Bethesda, MD).

### MECHANICAL TESTING

Compressive moduli of 1-month tissue constructs ($n = 4$) were determined in uniaxial stress-relaxation tests using a stepper motor-driven miniature compression device manufactured in-house with a miniature 5 mm DVRT® (Microstrain, Burlington, VT) used as a displacement gage in its linear range[26]. In brief, discs 3 mm in diameter and 1.5 mm thick were punched and trimmed from the central region of the construct. Discs were equilibrated in PBS containing protease inhibitors, placed in a cylindrical confining chamber filled with PBS, mounted in a miniature stepper motor controlled material testing machine, and compressed with a porous stainless steel platen. A 5% strain was applied and the load was monitored until equilibrium was reached followed by four 2% strain steps with stress relaxation between each. Data were recorded at a sampling rate of 10 points/s over a time increment of 480 s. Constructs were considered to fully relax during this increment based on a change in stress of less than 0.006 MPa over the final 180 s. The equilibrium modulus was then determined for each sample as the slope of the best linear regression fit ($r^2 > 0.99$) of the measured equilibrium stress vs applied strain.

### STATISTICAL ANALYSIS

We used a one-way analysis of variance (ANOVA) *F* test. Statistical analysis was performed with SPSS 13.0 statistical software (SPSS Inc., Chicago, IL). *P* values less than 0.05 were considered statistically significant.

## Results

### *IN VITRO* ENGINEERING OF SDSC-BASED TISSUE CONSTRUCTS IN A BIOREACTOR

After digestion with papain, the tissue constructs were still visible at days 0, 3, and 15, suggesting the presence of the PGA scaffolds. At day 31, the constructs disappeared, indicating complete degradation of the PGA scaffolds and replacement with newly formed tissue [Fig. 2(A)]. Biochemical analyses showed that DNA content per construct, an indicator of cell number, decreased with time [Fig. 2(B)]. In contrast, GAG content, a major matrix constituent associated with cartilage compressive stress, increased in a time-dependent manner [Fig. 2(C)]. The ratio of GAG to DNA, a chondrogenic differentiation index, increased over time up to day 31 [Fig. 2(D)].

Our western-blot data [Fig. 2(E)] showed that collagen II, another major matrix constituent associated with cartilage tension, was not detectable at day 3. However, collagen type II was detected at day 15 and increased rapidly until day 31, which was consistent with GAG expression [Fig. 2(C, D)]. After incubation in a differentiative growth factor cocktail supplemented bioreactor, tissue constructs at day 3 expressed the highest levels of Sox 9, a key chondrogenic transcription factor. With the maturation of tissue constructs, the expression of Sox 9 decreased in a time-dependent fashion.

Histology data [Fig. 2(F)] showed that day 31 constructs were filled with chondrocyte-occupied lacunae surrounded by Safranin O stained GAG [Fig. 2($f_1$)] and immunostained collagen II [Fig. 2($f_2$)]. As an early stage marker of cartilage development, collagen I was visible throughout the constructs [Fig. 2($f_3$)]. In addition, macrophages (type

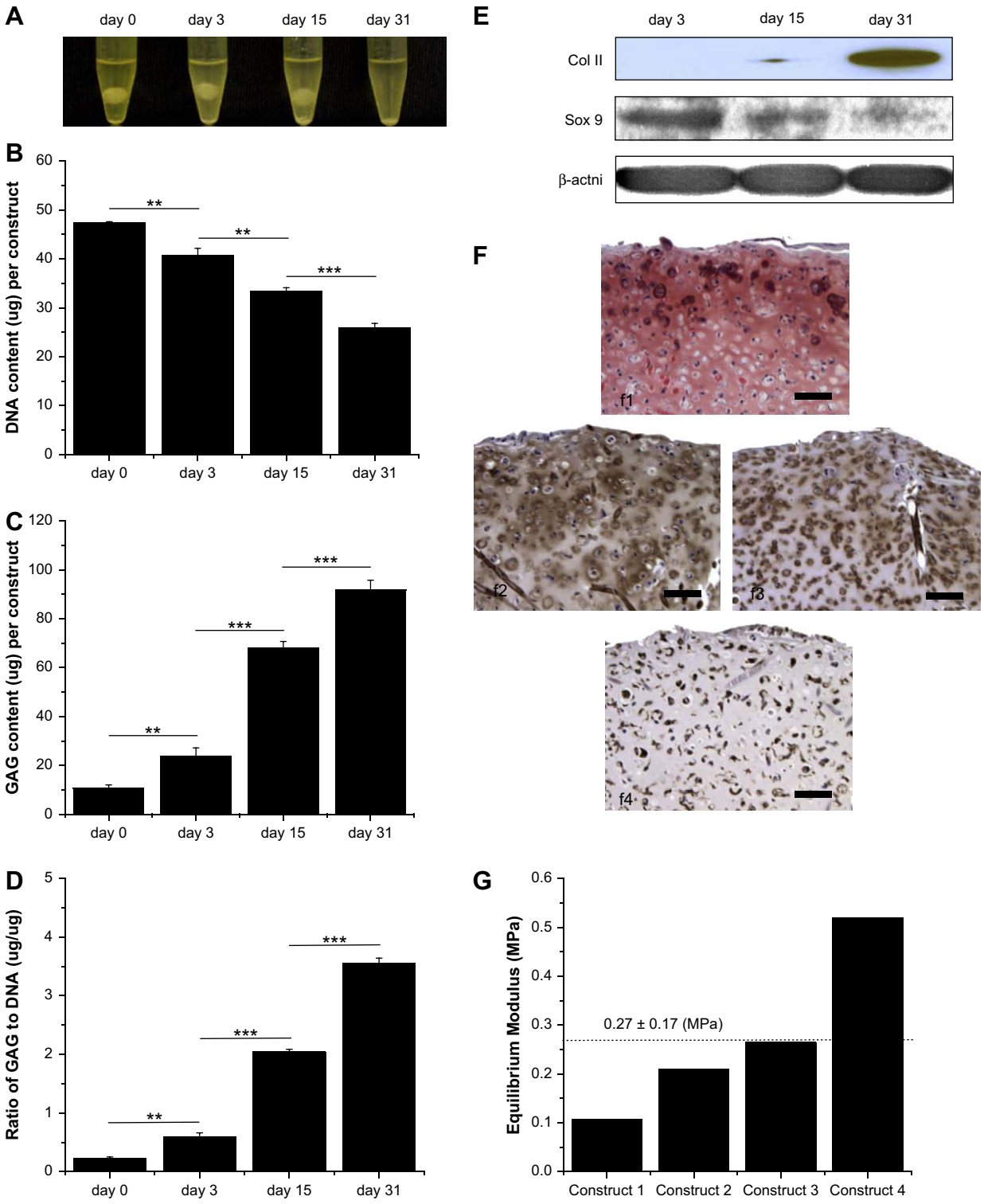


Fig. 2. *In vitro* SDSC-based tissue constructs. After papain digestion, the digests (A) from each construct were analyzed for DNA content (B) and GAG content (C). The chondrogenic index was shown as a ratio of GAG to DNA (D). Differences between time points are indicated as follows: $^{*}P < 0.05$; $^{**}P < 0.01$; and $^{***}P < 0.001$. Data are shown as average $\pm$ SD for $n = 4$. Protein expressions of collagen II and Sox 9 (E) were evaluated using western blots of constructs cultured for 3, 15, and 31 days. Histology (F) was used to evaluate marker gene expression with Safranin O stain for sulfated GAG ($f_1$) and immunostaining for collagen II ($f_2$), collagen I ($f_3$), and macrophages ($f_4$). Scale bars are 200 $\mu$m. Equilibrium modulus (G) was measured from four randomly selected constructs after 1 month of *in vitro* cultivation. The dotted line shows average $\pm$ SD for all four constructs.

A synovial cells) were detectable even after 28-day-differentiation in a bioreactor [Fig. 2($f_4$)]. The mechanical properties of bioreactor-engineered tissue constructs were also measured. Our data showed that the average equilibrium modulus of four tissue constructs at day 31 was 0.27 MPa [Fig. 2(G)], which is about one third of the native cartilage value[27].

*IN VIVO* IMPLANTATION OF PREMATURE TISSUE FOR THE REPAIR OF FULL-THICKNESS CARTILAGE DEFECTS

Three weeks after implantation, compared to the Empty group [Fig. 3($C_2$, $C_1$)], there was abundant expression of collagen II [Fig. 3($A_2$)] and less collagen I [Fig. 3($A_1$)] in the peripheral zone of the Construct group, which integrated well

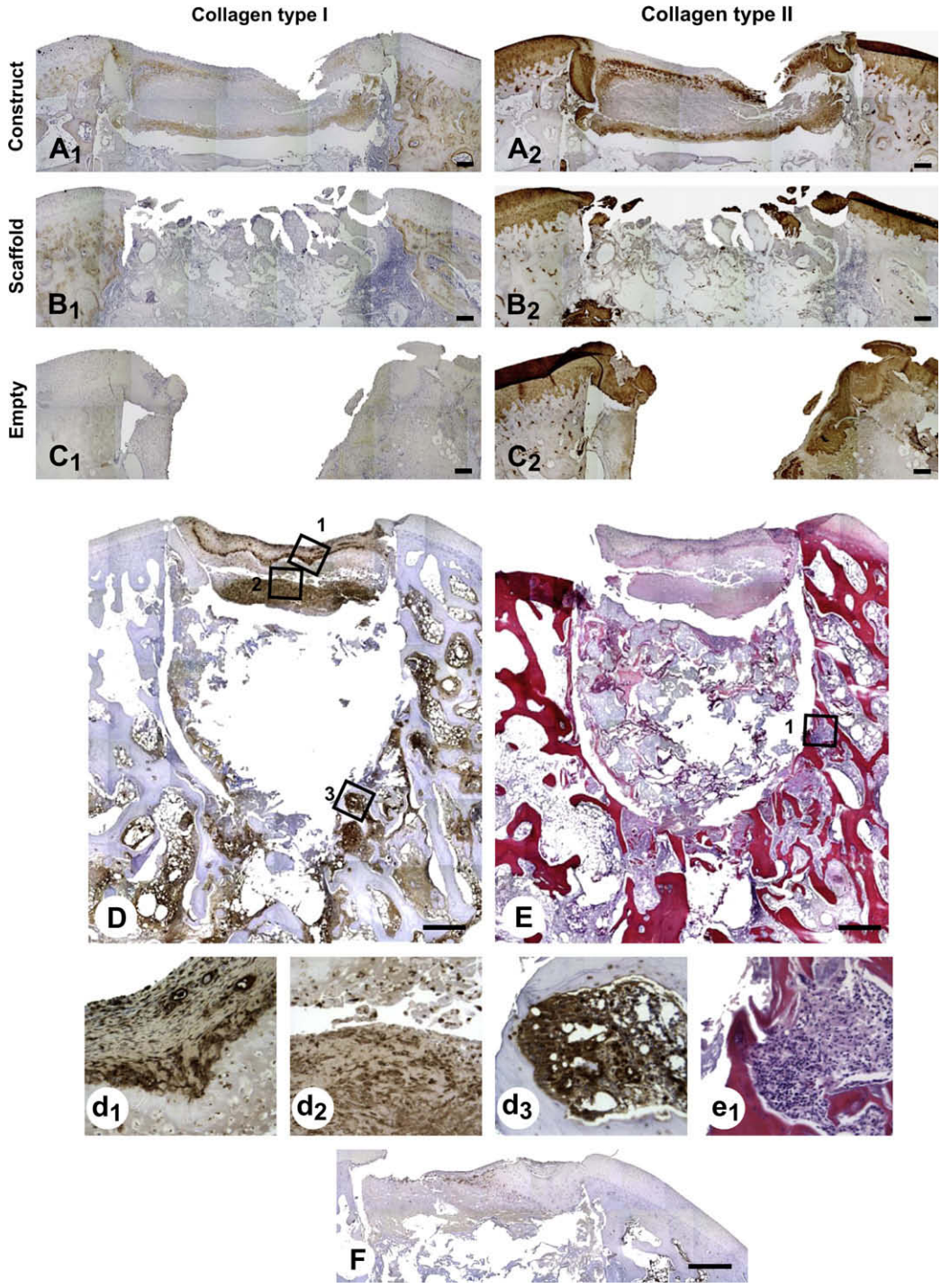


Fig. 3. Three weeks after implantation, immunostaining was performed for protein expression of collagen I ($A_1$, $B_1$, $C_1$) and collagen II ($A_2$, $B_2$, $C_2$) as well as macrophages (D, $d_1$, $d_2$, $d_3$, F), and H&E staining (E) for lymph cells ($e_1$) in Construct group ($A_1$, $A_2$, D, $d_1$, $d_2$, $d_3$) and Scaffold group ($B_1$, $B_2$, F) as well as Empty group ($C_1$, $C_2$). Enlargements ($d_1$, $d_2$) are from Fig. 3(D) in the implanted tissue constructs; and enlargements ($d_3$, $e_1$) are from Fig. 3(D, E), respectively, at the borderline between implanted Collagraft® and the surrounding native bone. All scale bars are 100 μm.

with the surrounding native cartilage [Fig. 3($A_1$, $A_2$)]. In contrast, there was a barely detectable expression of collagen I [Fig. 3($B_1$)] and collagen II [Fig. 3($B_2$)] in the Scaffold group. Part of the composites disappeared, likely a result of scaffold degradation. Immunostaining demonstrated that there were plenty of macrophages [Fig. 3(D)] located on both sides [Fig. 3($d_1$, $d_2$)] of the implanted tissue constructs and at the interface between fibrin glue-saturated Collagraft® and the adjacent native bone [Fig. 3($d_3$)], where there was an obvious gap full of lymphocytes [Fig. 3($e_1$)]. There were no macrophages detected in the Scaffold group [Fig. 3(F)].

At 6 months, the cartilage defects implanted with SDSC-based tissue constructs displayed a smooth and glistening surface [Fig. 4(A)] with expression of chondrogenic markers, sulfated GAG [Fig. 4($a_1$)], and collagen II [Fig. 4($a_2$)]; no collagen I was detectable [Fig. 4($a_3$)]. In contrast, the fibrin glue-saturated composite Scaffold group displayed obvious defects [Fig. 4(B)]. There was no sulfated GAG [Fig. 4($b_1$)], less collagen II [Fig. 4($b_2$)], and more collagen I [Fig. 4($b_3$)]. Defects in the Empty group were filled with rough whitish tissue [Fig. 4(C)] without sulfated GAG [Fig. 4($c_1$)] and with a mixture of collagen II [Fig. 4($c_2$)] and collagen I [Fig. 4($c_1$)]. Six months after transplantation, our results [Fig. 4(D)] showed that the mean histological score in the Construct group ($5.50 \pm 1.38$) was better than that of the Empty group ($8.25 \pm 0.50$). The Scaffold control group ($11.14 \pm 1.68$) had the highest score indicating the worst outcome.

## Discussion

The aim of this study was to evaluate the feasibility of allogeneic transplantation for the repair of osteochondral

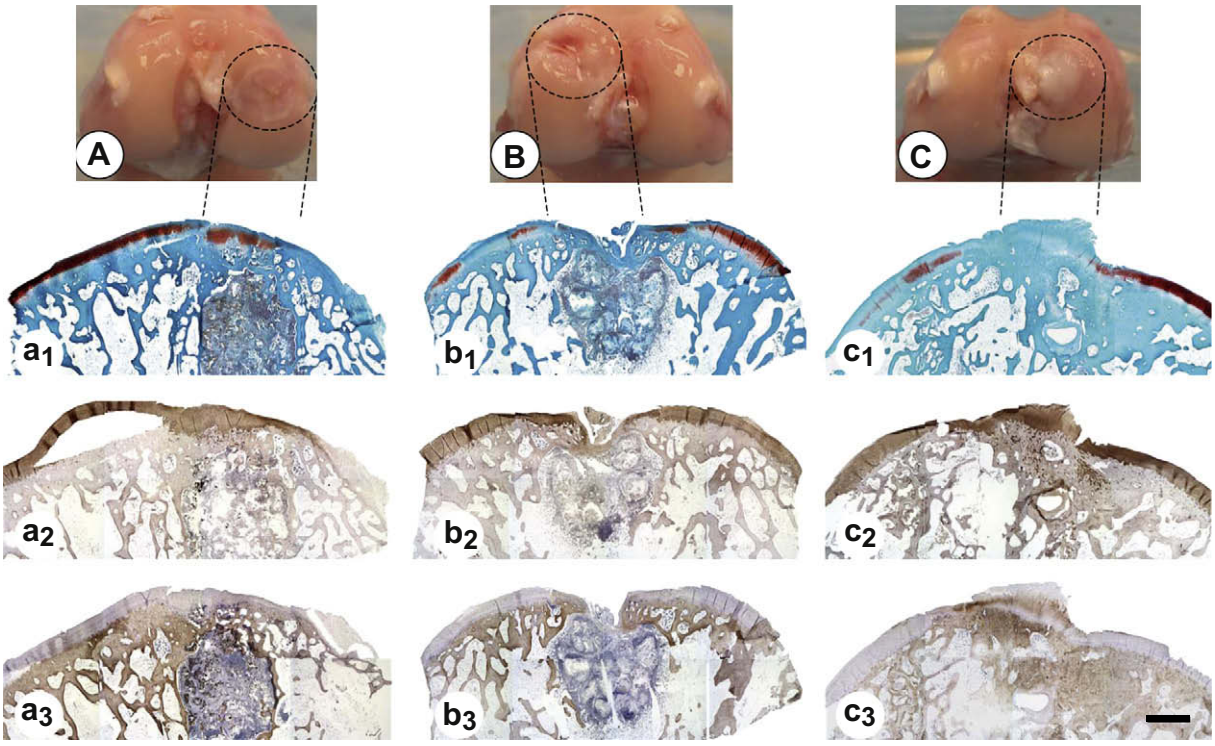


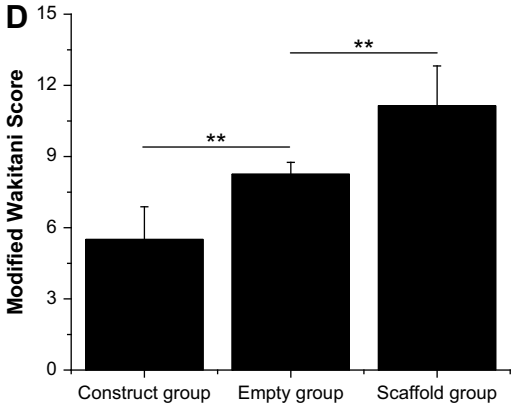


Fig. 4. Six months after implantation, the Construct group (A) was compared to the Scaffold group (B) and Empty group (C). Safranin O stain was for sulfated GAG ($a_1$, $b_1$, $c_1$) and immunostaining was for protein expression of collagen II ($a_2$, $b_2$, $c_2$) and collagen I ($a_3$, $b_3$, $c_3$). All scale bars are 200 μm. The modified Wakitani Score (D) was used to evaluate the regeneration of repair tissue and integration with the surrounding native tissue.

defects using *in vitro* engineered SDSC-based tissue constructs. Our previous study demonstrated that SDSCs possessed high self-renewing capacity in the clonogenic growth format and SDSCs could be induced to differentiate toward adipogenesis, osteogenesis and chondrogenesis[22]. In this investigation, conventionally passaged SDSC-based cartilage tissue constructs were engineered by seeding a mixture of SDSCs and fibrin glue into PGA meshes followed by 1-month incubation in a serum-free culture system in the presence of growth factor cocktails. Six months after allogeneic transplantation with premature cartilage, rabbit femoral condyle full-thickness cartilage defects were resurfaced with hyaline-like cartilage that displayed good integration with the surrounding native cartilage.

Recently, stem cell-based tissue engineering has become a promising and fascinating biological approach for cartilage repair. Compared to other sources of MSCs, such as bone marrow[11], skeletal muscle[28], fat[29] and periosteum[30], SDSCs can offer some unique advantages for cartilage tissue engineering[10,15–21]. In our study, the biodegradable PGA mesh provides temporary mechanical support[31] and the fibrin glue acts to provide homogenous cell distribution and enhance *in vitro* chondrogenesis as well as potentially blocking rejection reactions[32]. Rotating bioreactors provide hydrodynamic culture conditions, which has been proven as an efficient three-dimensional culture method for cartilage tissue engineering[31]. Finally, serum-free defined medium with a growth factor cocktail can provide SDSCs with chemical signals for maximum cell proliferation and chondrogenic differentiation as previously reported[22].

After 1-month incubation in a bioreactor system, constructs became premature tissue in which expression of sulfated GAG and collagen II increased in a time-dependent manner. As an early chondrogenic marker, collagen I was still detectable up to 1 month, which is consistent with our previous studies[22,26]. Histology data indicated that many macrophages were found throughout tissue constructs, contradicting a previous study suggesting that passage 3 monolayer cultured SDSCs formed a homogeneous-appearing population of fibroblast-like cells negative for the expression of the macrophage-specific CD14 gene[20]. In contrast, our previous study[22,26] suggested that plastic adhesion could not remove macrophages, presumably due to macrophages being adhesion cells like fibroblasts. Negative selection proved to be a fast and simple method for the purification of SDSCs from mixed synovial cells by minimizing macrophages that might inhibit *in vitro* chondrogenesis. However, it is not known if contaminated macrophages also affect *in vivo* cartilage regeneration.

Although implantation of unmodified MSCs has been reported to repair cartilage defects in rabbits[25], the implantation of uncommitted cells often leads to fibrocartilage formation, indicating that the *in vivo* environment is not sufficient to promote chondrogenesis. In contrast, modified MSCs with adenovirus mediated-bone morphogenetic protein (BMP)-2 produced hyaline cartilage-like tissue after implantation in the knee joint, whereas uninfected MSCs either failed to fill up the defects or formed fibrous tissue mainly composed of type I collagen[3]. In our study, SDSC-based tissue constructs were implanted to repair rabbit femoral condyle cartilage defects. Three weeks after transplantation, the Construct group showed increasing collagen II and decreasing collagen I expression. At 6 months, the Construct group displayed real hyaline-like cartilage with intense expression of sulfated GAG and collagen II as well as no expression of collagen I, indicating that the damaged joint environment favors continuous differentiation and maturation of the implanted premature cartilage tissue, which is consistent with a previous report[33].

Full healing is a complex process and demands differentiation through natural signaling pathways as well as integration of the regenerated tissue with native tissues. Since inadequate cartilage integration may ultimately lead to fibrillation and degeneration of the surrounding tissue[34], one challenge in cartilage repair is to obtain the proper integration of a mechanically stable interface between repair and host tissues at the defects[35]. As documented, MSCs possess the capacity to engraft successfully into various tissues and organs and maintain long-term stability when infused systematically[36]. Even more, MSCs infused in the peripheral circulation have the ability to migrate to a specific site of injury. Our data demonstrated that there was good integration between the implanted tissue and the surrounding native cartilage 6 months after premature tissue construct implantation. Cartilage tissue integration can be affected by the differentiation and remodeling of the transplanted premature tissue cells. It is dependent on collagen synthesis and cross-linking maturation at the interface[37]. In this study, we observed that there was expression of macrophages in the implanted constructs at 3 weeks that disappeared 6 months after implantation, presumably indicating macrophages may be involved in the remodeling and integration of newly formed cartilage.

Since most patients with advanced osteoarthritis are elderly, many findings indicate an age-related decrease affecting the amount[38], and proliferative potential of MSCs[39], as well as the chondrogenic differentiation capability of MSCs[40]. Currently, there are several reports describing the clinical use of allogeneic donor-mismatched MSCs without host immune rejection or incidence of graft-versus-host disease[41,42]. Apart from the possibility of therapeutic use of allogeneic MSCs in immunocompetent patients without obvious immune rejection, allogeneic MSCs could possibly allow therapeutic delivery in a limited time period from healthier and younger donors. There is no donor site morbidity involved in the use of allogeneic MSCs. Koga *et al.* transplanted undifferentiated SDSCs into a full-thickness articular cartilage defect and did not observe features of immune reactions with the use of allogeneic cells[43]. Our study also demonstrated that allogeneic MSCs could survive *in vivo* even after they differentiated into chondrocytes *in vitro*. The use of allogeneic stem cells could allow manufacturing of certified cell batches ready for implantation, circumventing the limitations and patient-to-patient variability of autologous cell protocols.

Another concern for cartilage injury treatment is found in a study that the cartilage became thinner at 24 weeks and the tidemark moved upward over the majority of the repair zone, likely due to the dedifferentiation of MSCs to fibrocartilage (marked by the expression of collagen I) or maturation to hypertrophic cartilage (as indicated by the expression of collagen X)[43]. This is a general phenomenon seen in cartilage repair of osteochondral defects[25,44]. Violation of the tidemark and the subchondral plate presents a problem with restoration of the original tidemark, which is also seen in humans and has been described in microfracture[45]. In the current study, we could not detect collagen I as well as collagen X (data not shown) in the newly formed tissue, indicating a stable hyaline phenotype of the resurfacing cartilage.

Our study demonstrates that allogeneic SDSC-based tissue constructs can be used to repair femoral condyle osteochondral defects. However, we also observed some limitations in this study. As a bone substitute, Collagraft®

was shown to induce long-term inflammation that interfered with osteochondral regeneration resulting in the repair of the Scaffold group being worse than that of the Empty group. In addition, the lack of reestablishing normal subchondral bone architecture and the lack of resorption or remodeling of the Collagraft® might result in inferior mechanical properties in the newly formed cartilage. Our long-term goal is to engineer a high-quality cartilage substitute using allogeneic SDSCs for clinical repair of cartilage defects. Thus, further investigations need to be performed in the future.

## Conflict of interest

All authors disclose any financial and personal relationships with other people or organizations that could inappropriately influence (bias) this work, including employment, consultancies, stock ownership, honoraria, paid expert testimony, patent applications/registrations, and grants or other funding.

## Acknowledgments

We thank Suzanne Smith and Mark Shoukry for editing the manuscript and Nina Clovis for technical support.

### References

1. Buckwalter JA. Articular cartilage: injuries and potential for healing. J Orthop Sports Phys Ther 1998;28:192–202.
2. Hunziker EB. Articular cartilage repair: are the intrinsic biological constraints undermining this process insuperable? Osteoarthritis Cartilage 1999;7:15–28.
3. Gelse K, von der Mark K, Aigner T, Park J, Schneider H. Articular cartilage repair by gene therapy using growth factor-producing mesenchymal cells. Arthritis Rheum 2003;48:430–41.
4. Nehrer S, Spector M, Minas T. Histologic analysis of tissue after failed cartilage repair procedures. Clin Orthop Relat Res 1999;365: 149–62.
5. Lee CR, Grodzinsky AJ, Hsu HP, Spector M. Effects of a cultured autologous chondrocyte-seeded type II collagen scaffold on the healing of a chondral defect in a canine model. J Orthop Res 2003;21: 272–81.
6. Schaefer D, Martin I, Jundt G, Seidel J, Heberer M, Grodzinsky A, *et al*. Tissue-engineered composites for the repair of large osteochondral defects. Arthritis Rheum 2002;46:2524–34.
7. Obradovic B, Martin I, Padera RF, Treppo S, Freed LE, Vunjak-Novakovic G. Integration of engineered cartilage. J Orthop Res 2001;19:1089–97.
8. Vunjak-Novakovic G. The fundamental of tissue engineering: scaffold and bioreactors. In: Bock G, Goode J, Eds. Tissue Engineering of Cartilage and Bone. John Wiley & Sons Publication; 2002:34–46. Novartis Foundation Symposium 249.
9. Hui JH, Chen F, Thambyah A, Lee EH. Treatment of chondral lesions in advanced osteochondritis dissecans: a comparative study of the efficacy of chondrocytes, mesenchymal stem cells, periosteal graft, and mosaicplasty (osteochondral autograft) in animal models. J Pediatr Orthop 2004;24:427–33.
10. Hunziker EB, Rosenberg LC. Repair of partial-thickness defects in articular cartilage: cell recruitment from the synovial membrane. J Bone Joint Surg Am 1996;78:721–33.
11. Pittenger MF, Mackay AM, Beck SC, Jaiswal RK, Douglas R, Mosca JD, *et al*. Multilineage potential of adult human mesenchymal stem cells. Science 1999;284:143–7.
12. Barry FP, Murphy JM, English K, Mahon BP. Immunogenicity of adult mesenchymal stem cells: lessons from the fetal allograft. Stem Cells Dev 2005;14:252–65.
13. Le Blanc K, Ringdén O. Immunomodulation by mesenchymal stem cells and clinical experience. J Intern Med 2007;262:509–25.
14. Sekiya I, Larson BL, Smith JR, Pochampally R, Cui JG, Prockop DJ. Expansion of human adult stem cells from bone marrow stroma: conditions that maximize the yields of early progenitors and evaluate their quality. Stem Cells 2002;20:530–41.
15. De Bari C, Dell'Accio F, Karystinou A, Guillot PV, Fisk NM, Jones EA, *et al*. A biomarker-based mathematical model to predict bone-forming potency of human synovial and periosteal mesenchymal stem cells. Arthritis Rheum 2008;58:240–50.
16. Mochizuki T, Muneta T, Sakaguchi Y, Nimura A, Yokoyama A, Koga H, *et al*. Higher chondrogenic potential of fibrous synovium- and adipose synovium-derived cells compared with subcutaneous fat-derived cells: distinguishing properties of mesenchymal stem cells in humans. Arthritis Rheum 2006;54:843–53.
17. Sakaguchi Y, Sekiya I, Yagishita K, Muneta T. Comparison of human stem cells derived from various mesenchymal tissues: superiority of synovium as a cell source. Arthritis Rheum 2005;52:2521–9.
18. Yoshimura H, Muneta T, Nimura A, Yokoyama A, Koga H, Sekiya I. Comparison of rat mesenchymal stem cells derived from bone marrow, synovium, periosteum, adipose tissue, and muscle. Cell Tissue Res 2007;327:449–62.
19. Hunziker EB. Growth-factor-induced healing of partial-thickness defects in adult articular cartilage. Osteoarthritis Cartilage 2001;9:22–32.
20. De Bari C, Dell'Accio F, Tylzanowski P, Luyten FP. Multipotent mesenchymal stem cells from adult human synovial membrane. Arthritis Rheum 2001;44:1928–42.
21. Jo CH, Ahn HJ, Kim HJ, Seong SC, Lee MC. Surface characterization and chondrogenic differentiation of mesenchymal stromal cells derived from synovium. Cytotherapy 2007;9:316–27.
22. Pei M, He F, Vunjak-Novakovic G. Synovium-derived stem cell-based chondrogenesis. Differentiation 2008;76:1044–56.
23. Pineda S, Pollack A, Stevenson S, Goldberg V, Caplan A. A semiquantitative scale for histologic grading of articular cartilage repair. Acta Anat (Basel) 1992;143:335–40.
24. Wakitani S, Goto T, Pineda SJ, Young RG, Mansour JM, Caplan AI, *et al*. Mesenchymal cell-based repair of large, full-thickness defects of articular cartilage. J Bone Joint Surg Am 1994;76:579–92.
25. Sellers RS, Peluso D, Morris EA. The effect of recombinant human bone morphogenetic protein-2 (rhBMP-2) on the healing of full-thickness defects of articular cartilage. J Bone Joint Surg Am 1997;79: 1452–63.
26. Pei M, He F, Kish V, Vunjak-Novakovic G. Engineering of functional cartilage tissue using stem cells from synovial lining: a preliminary study. Clin Orthop Relat Res 2008;466:1880–9.
27. Chen AC, Bae WC, Schinagl RM, Sah RL. Depth- and strain-dependent mechanical and electromechanical properties of full-thickness bovine articular cartilage in confined compression. J Biomech 2001;34:1–12.
28. Deasy BM, Jankowski RJ, Huard J. Muscle-derived stem cells: characterization and potential for cell-mediated therapy. Blood Cells Mol Dis 2001;27:924–33.
29. Zuk PA, Zhu M, Mizuno H, Huang J, Futrell JW, Katz AJ, *et al*. Multilineage cells from human adipose tissue: implications for cell-based therapies. Tissue Eng 2001;7:211–28.
30. De Bari C, Dell'Accio F, Luyten FP. Human periosteum-derived cells maintain phenotypic stability and chondrogenic potential throughout expansion regardless of donor age. Arthritis Rheum 2001;44:85–95.
31. Pei M, Solchaga LA, Seidel J, Zeng L, Vunjak-Novakovic G, Caplan AI, *et al*. Bioreactors mediate the effectiveness of tissue engineering scaffolds. FASEB J 2002;16:1691–4.
32. Kreder HJ, Moran M, Keeley FW, Salter RB. Biologic resurfacing of a major joint defect with cryopreserved allogeneic periosteum under the influence of continuous passive motion in a rabbit model. Clin Orthop Relat Res 1994;300:288–96.
33. Shapiro F, Koide S, Glimcher MJ. Cell origin and differentiation in the repair of full-thickness defects of articular cartilage. J Bone Joint Surg Am 1993;75:532–53.
34. Ghadially JA, Ghadially R, Ghadially FN. Long-term results of deep defects in articular cartilage. A scanning electron microscope study. Virchows Arch B Cell Pathol 1977;25:125–36.
35. Reindel ES, Ayroso AM, Chen AC, Chun DM, Schinagl RM, Sah RL. Integrative repair of articular cartilage in vitro: adhesive strength of the interface region. J Orthop Res 1995;13:751–60.
36. Devine SM, Hoffman R. Role of mesenchymal stem cells in hematopoietic stem cell transplantation. Curr Opin Hematol 2000;7:358–63.
37. Williamson AK, Masuda K, Thonar EJ, Sah RL. Growth of immature articular cartilage in vitro: correlated variation in tensile biomechanical and collagen network properties. Tissue Eng 2003;9:625–34.
38. Fibbe WE, Noort WA. Mesenchymal stem cells and hematopoietic stem cell transplantation. Ann N Y Acad Sci 2003;996:235–44.
39. Tanaka H, Ogasa H, Barnes J, Liang CT. Actions of bFGF on mitogenic activity and lineage expression in rat osteoprogenitor cells: effect of age. Mol Cell Endocrinol 1999;150:1–10.
40. Fiorito S, Magrini L, Adrey J, Mailhé D, Brouty-Boyé D. Inflammatory status and cartilage regenerative potential of synovial fibroblasts from patients with osteoarthritis and chondropathy. Rheumatology (Oxford) 2005;44:164–71.
41. Barry FP, Murphy JM. Mesenchymal stem cells: clinical applications and biological characterization. Int J Biochem Cell Biol 2004;36:568–84.
42. Horwitz EM, Prockop DJ, Fitzpatrick LA, Koo WW, Gordon PL, Neel M, *et al*. Transplantability and therapeutic effects of bone marrow-derived

mesenchymal cells in children with osteogenesis imperfecta. Nat Med 1999;5:309–13.
43. Koga H, Muneta T, Ju YJ, Nagase T, Nimura A, Mochizuki T, *et al*. Synovial stem cells are regionally specified according to local microenvironments after implantation for cartilage regeneration. Stem Cells 2007;25:689–96.
44. Adachi N, Sato K, Usas A, Fu FH, Ochi M, Han CW, *et al*. Muscle derived, cell based ex vivo gene therapy for treatment of full thickness articular cartilage defects. J Rheumatol 2002;29:1920–30.
45. Brown WE, Potter HG, Marx RG, Wickiewicz TL, Warren RF. Magnetic resonance imaging appearance of cartilage repair in the knee. Clin Orthop Relat Res 2004;422:214–23.